Temperature dependence of dielectric soil moisture measurement in an Internet of Things system – a case study

Andrzej Wilczek[1] , *Marcin Kafarski*[1] , *Jacek Majcher*[2] , *Agnieszka Szypłowska*[1] , *Małgorzata Budzeń*[1],
Arkadiusz Lewandowski[3] , *Artur Nosalewicz*[1] , *and Wojciech Skierucha*[1]*

[1]Institute of Agrophysics, Polish Academy of Sciences, Doświadczalna 4, 20-290 Lublin, Poland
[2]Department of Electrical Engineering and Electrotechnologies, Lublin University of Technology, Nadbystrzycka 38A,
20-618 Lublin, Poland
[3]Institute of Electronic Systems, Warsaw University of Technology, Nowowiejska 15/19, 00-665 Warsaw, Poland

Abstract. Soil moisture is a key parameter in determining crop growth and yield. Modern agriculture does not only take into account soil moisture measurements obtained once at selected points in the field, but also focuses on moisture monitoring. Knowledge of the variability over time and analysis of the variation in readings caused by heavy rainfall or strong sunshine and high soil temperature changes is very important for future modelling, prediction and automated irrigation. The aim of this paper is to present a developed soil moisture monitoring system for a soil profile up to 34 cm depth incorporating Internet of Things technologies. The system was built based on an eight-channel time domain reflectometer to measure soil moisture based on dielectric properties. The developed system integrates both dielectric moisture measurement and innovative web-based server and visualisation services. The autonomous station was equipped with a long-range wireless communication and a solar-charged battery. Analysis of the results enabled us to observe the subtle deviations of moisture content of the upper soil layer during diurnal cycles. The designed station can be used in the future to integrate a high accuracy automatic field irrigation system and acquire data for precision agriculture.

Keywords: soil moisture monitoring, dielectric permittivity, time domain reflectometry, wireless communication, Internet of Things

1. INTRODUCTION

Soil water content is one of the most important environmental variables, affecting plant growth and crop yield. In agriculture, accurate assessment of soil water content is important for making production decisions, adjusting the dates of respective treatments and processes, and for optimizing irrigation scheduling and its automation (Cepuder and Nolz 2007; Gałęzewski *et al.,* 2021). Continuous monitoring of soil moisture in a soil profile may be especially beneficial in precision agriculture and in conditions requiring sustainable and efficient use of water resources. Soil water content is also a crucial parameter in vadose zone hydrology (Vereecken *et al.,* 2008).

There are multiple methods and devices used for soil moisture measurement (Robinson *et al.,* 2008). Dielectric sensors are a promising and popular choice for moisture monitoring in soil profile due to numerous advantages including ease-of-use, environmental safety, and ease of measurement automation. Measurement accuracy of a given dielectric sensor depends on its exact principle of operation, frequency, specific construction and the applied

*Corresponding author e-mail: w.skierucha@ipan.lublin.pl

calibration function. Generally, the most accurate and usually the most expensive sensors operate in the time domain and do not require soil-specific calibration in common mineral soils. However, due to various soil properties influencing relations between soil volumetric water content and its dielectric properties, the readout of the dielectric sensors may be affected by some interfering factors, such as soil texture, salinity and temperature (Gong *et al.*, 2003; Chen and Or, 2006). The above-mentioned factors may pose problems especially for low-cost capacitance/impedance sensors operating at frequencies of tens of MHz or lower. The usual solution is to apply calibration curves developed for a given soil type or to perform soil-specific calibration of the sensor (Vaz *et al.,* 2013). The influence of temperature on soil dielectric permittivity is a more complicated problem, as it stems from several competing mechanisms that include the impact of temperature on dielectric permittivity of free water, release of bound or confined water into the free water phase, and the impact of temperature on various interphase phenomena and ionic conductivity (Or and Wraith 1999; Skierucha 2009; Wagner *et al.,* 2011; Szypłowska *et al.,* 2023). Therefore, depending on the texture and water content of a given soil, the real part (ε') of complex dielectric permittivity or apparent permittivity (ε_a) may either rise, decrease or remain constant with an increase in temperature. Moreover, in the case of the real part of dielectric permittivity, the influence of temperature may depend on frequency, *i.e.* at frequencies of tens of MHz ε' might increase with the increase in temperature, while at several hundreds of MHz it may decrease with the increase in temperature. This might make is a challenging task to implement in the sensor's firmware a general correction for the soil-permittivity temperature dependence. In addition to factors directly influencing soil complex dielectric permittivity and its relation to soil moisture, the accurate interpretation of soil moisture data, especially for agricultural purposes, should also take into account the impact of the method of tillage on the dynamics of soil moisture and temperature (Gałęzewski *et al.,* 2022).

Dielectric sensors can be used as hand-held devices for point measurements, placed on mobile platforms for on-the-go sensing or installed at specific locations as parts of automatic monitoring stations. Sensor readings can be taken directly for a given agricultural, environmental or scientific application or used as a basis for calibration and validation of remote sensing performed by airborne or satellite platforms. Regardless of the specific application, issues relating to the availability, assimilation and processing of the obtained data are of high importance. Therefore, many of the modern sensors are developed and implemented as parts of a network enabling remote data upload with an included web service for data storage, processing and visualization. In Ullah *et al.* (2021) an IoT platform with soil moisture sensors was proposed as a water- and energy-efficient smart irrigation system. Goap *et al.* (2018)

presented an IoT irrigation control system that collected physical parameters from field measurements, including soil moisture and temperature, air temperature and humidity, integrated the obtained data with weather forecast from a web service and processed the information with the use of machine learning techniques. Another recent implementation of Internet of Things framework for soil moisture monitoring is presented in Tan *et al.* (2022), where soil moisture readings were collected by a Raspberry Pi unit and sent to a cloud server and simultaneously used for irrigation water pump control.

The aim of the paper is to present the soil moisture and temperature monitoring system utilizing time-domain-reflectometry (TDR) probes placed in an automatic monitoring station connected to an IoT service. Data collected during several weeks has been analyzed with special emphasis on the diurnal changes of the volumetric water content readings and their correlation with soil temperature.

2. MATERIALS AND METHODS

2.1. Installation

The measurement system was installed in a field site located near Lublin, Poland, on uncultivated soil covered with periodically mowed grass, in the vicinity of fruit trees. The soil was of the luvisol type, originated from loess. Eight FP/mts field type TDR probes (E-Test Sp. z o.o., Poland, e-test.eu) were installed in an excavated hole. After the installation procedure, this hole was carefully filled with the same soil to minimise disturbance to the soil profile structure. The TDR probes were placed in the undisturbed soil at four depths of 5, 13, 21, and 34 cm. Two probes were installed at each level (Fig. 1c). The maximum depth of the probe installation was chosen to cover the arable layers and subsoil. The installation depths are not uniformly distributed in order to be able to better study dynamic soil processes. The probes were connected to an eight-channel TDR/MUX meter controlled by a wireless cloud data logger (Fig. 1a). The TDR meter, logger and solar-charged battery were enclosed in a metal box to protect it from harsh environmental conditions (Fig. 1b). Data from the logger was transmitted wirelessly to an IoT server for data collection and visualization on a website. The measurement system was installed in Stasin, Poland at coordinates 51.212 N, 22.465 E. The description of the TDR/MUX meter and FP/mts probes were presented in (Skierucha *et al.,* 2012).

2.2. LoRaWAN wireless data logger

The logger is built based on the PYCOM LoPy4 module (https://pycom.io). Its programming is conducted in the MicroPython language and does not require a compiler. The device can communicate locally with TDR/MUX *via* the built-in RS-485 or SDI-12 interface (González-Teruel *et al.,* 2019). The device operates completely maintenance-free. Its installation consists of connecting the interface and
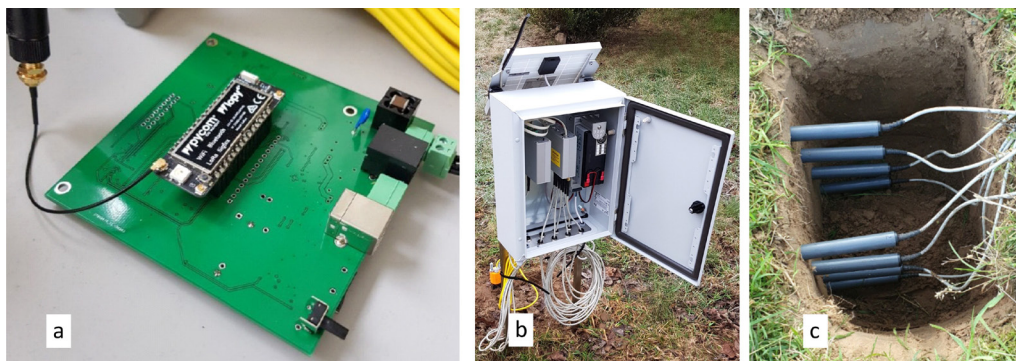
Fig. 1. Field Installation of LoRaWAN IoT system: a) Wireless Data Logger, b) installed measurement station, c) TDR probes in the soil profile.
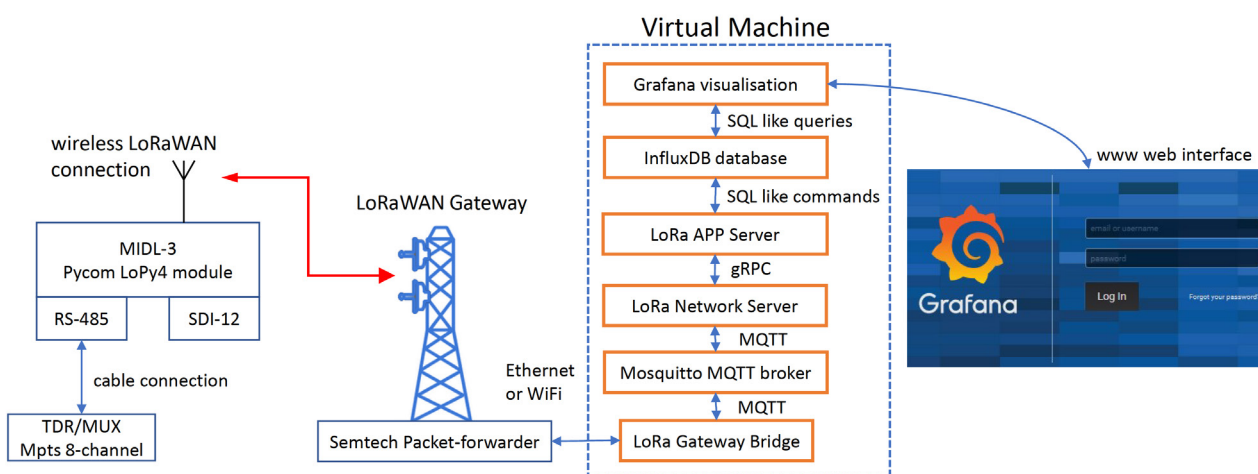
Fig. 2. LoRa WAN solution with server services and Internet browser-based visualisation.

power cables. After power-up, the device performs auto-configuration, checking the channels from which it receives the valid readings of moisture, temperature and electrical conductivity. From this moment, measurements are made only in these channels. Change in the channel configuration requires device reset by pressing the RESET button. The logger is powered by a 12 V gel battery with a capacity of 7.2 Ah, which is sufficient for one year of operation without additional charging. For wireless communication, the logger uses the LoRa WAN standard widely recognised worldwide for long-range data transmission up to 10 km in rural undeveloped areas. The logger is programmed with two unique 16 byte session keys needed to encrypt communications. These keys are needed when the logger is activated on the server.

2.3. Server services and visualisation features

In order to efficiently and securely collect monitoring data, a commercially available virtual machine (VM) on Google Cloud Platform (GCP) was used as the server. A standard single-processor instance with 3.75 GB of RAM and 10 GB of disk space was selected. A fixed IP address was set to avoid domain redirection issues. The server was based on the Linux operating system version Debian 9 "Stretch" release. The LoRa Gateway Bridge to the Message Queues Telemetry Transport (MQTT) service was installed along with the MQTT broker "Mosquitto". The LoRaWAN (Correia *et al.,* 2023) network server and application server were then installed. The task of the network server and application server is to establish a secure AES-128 encrypted connection to Kerlink's Wirnet iStation Gateway (Pinelo *et al.,* 2023) and then to the soil monitoring station logger. The whole system checks the correctness of the two-way communication, removes duplicate data packets, adjusts the wireless transmission rate and sends a return acknowledgement of packet receipt from the monitoring station. The connection structure of the entire system is presented in Fig. 2. The measurement results are collected in the InfluxDB (Nasar and Kausar, 2019) database for collecting time series.

Visualisation is based on the modern Grafana (Cicioğlu and Çalhan, 2021) service, which is also installed on the Google VM. It allows full permission management, inviting new users and automatic password recovery. The developed

system has been equipped with a notification mechanism for critical situations, such as no flow of data for more than a few hours, excessively discharged battery or exceeding the pre-set value of probe temperature or moisture. It now has an email account from which it can send notifications defined by editors. The generated notifications can contain precise information about the cause of the event along with a description of the situation in the form of graphs. Thanks to the use of two-way communication, it is possible to remotely change the measurement interval, which helps in the winter period, where there is a solar energy deficit, to keep the system running smoothly. Current tests indicate that the system may be useful for further development targeting automation in precision agriculture.

3. RESULTS AND DISCUSSION

Data from the system has been collected since 2020. For the illustrative purposes of this paper, the period from 6 May to 15 June 2023 was selected for visualisation. Figure 3a presents soil moisture data collected at four soil depths, while Fig. 3b shows moisture and temperature data obtained

at 5 cm depth, where the changes were more dynamic than in the deeper layers of the soil profile. The recorded data shows that rainfall occurred three times during this period. Measurements were taken every 2.5 min. To analyse the thermal dependencies, data collected over a one-week period from 8 to 15 May 2023 were used, which constituted approximately 4,000 measurements. These measurements were recorded after rainfall, which is visible on the graph as a sharp increase in moisture content. It was important that this was the greatest change in moisture content and a slow decrease with the greatest possible variation in temperature, which is most evident in the measurements at a depth of 5 cm.

3.1. Analysis of the moisture and temperature variations

The changes in soil moisture in the selected time window was presented in Fig. 4. One can see that the moisture content did not monotonically decrease, but exhibited a diurnal pattern with periods of increase and decrease. A general trend of decreasing moisture was approximated by a third-degree polynomial fitted to the selected time
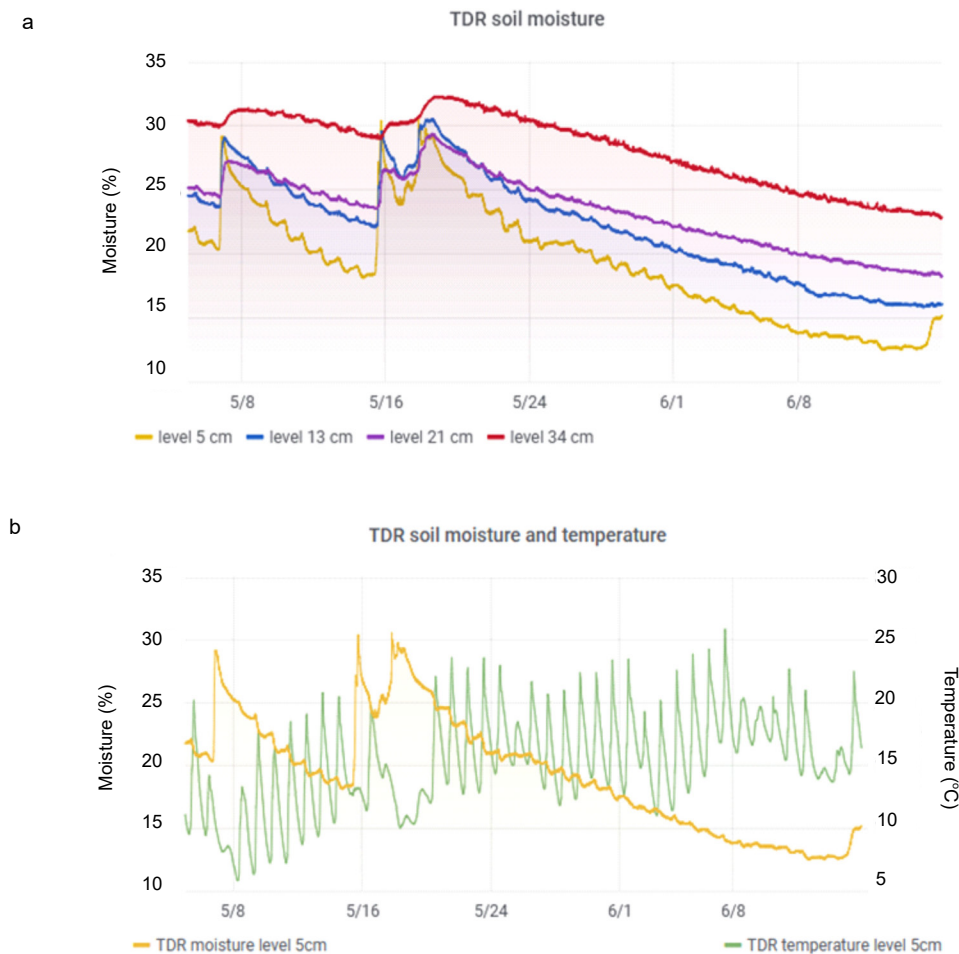
Fig. 3. Screenshot of the Grafana website for the selected period after rainfall, a) moisture data collected at four soil depths, b) moisture and temperature collected at 5 cm depth.
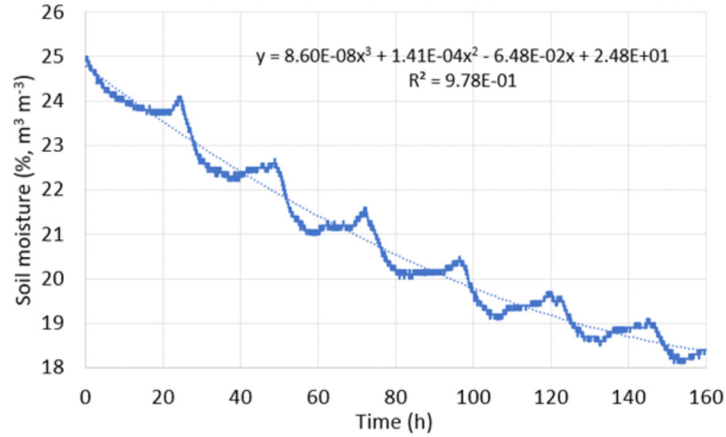
**Fig. 4.** Selected seven-day period of soil moisture decrease after rainfall.

range, which enabled to evaluate the diurnal moisture variations (Fig. 4). The polynomial acts as a low band filter to determine the actual change in moisture content. From the difference between the actual measured data (θ_{means}) and the moisture determined at a given time from the fitted polynomial (θ_{model}), the moisture deviation was determined according to relation: $\delta\theta = \theta_{means} - \theta_{model}$. This deviation, shown in Fig. 5, depends on the variation of soil dielectric permittivity with temperature but can also be caused by an uneven evaporation rate from the soil surface. The same graph also shows the changes in soil temperature measured at the 5 cm depth. Maxima (odd number) and minima (even number) of temperature were marked on the graph. These allowed to determine moisture deviation coefficient (M_{dc}) of $\delta\theta$, which was calculated according to the following relation:

$$M_{dc} = \frac{M_{n+1} - M_n}{T_{n+1} - T_n}, n = 1...2,$$

where: M_n were consecutive minima (n odd) and maxima (n even) of $\delta\theta$ and T_n were consecutive maxima (n odd) and minima (n even) of temperature, closest in time to respective M_n. For example, if temperature rose in the diurnal cycle by 11.1°C (T2 and T3 points in Fig. 5), and in the same cycle moisture decreased by 1.05% (M2 and M3 points in Fig. 5), the value of M_{dc} for the given cycle was calculated according to equation giving -0.095 %/°C. For the whole data range, 12 of these moisture deviation coefficients were calculated and then correlated with the moisture content values obtained from the model in the middle of the timespan of a given cycle, which was taken as the average moisture value in the cycle. The relation between M_{dc} and moisture content was presented in Fig. 6.
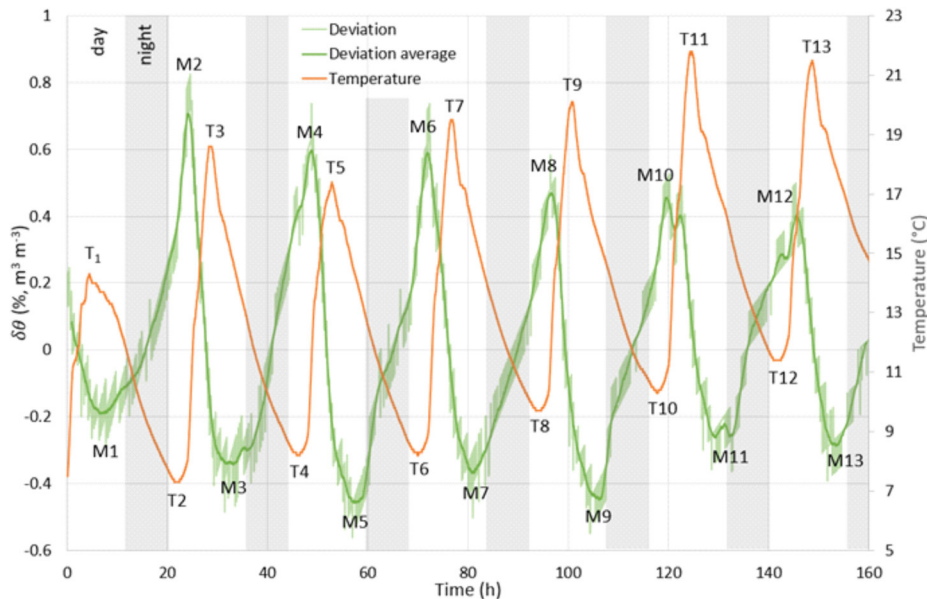
Fig. 5. Moisture deviation $\delta\theta$ in relation to soil temperature in the analysed time period.
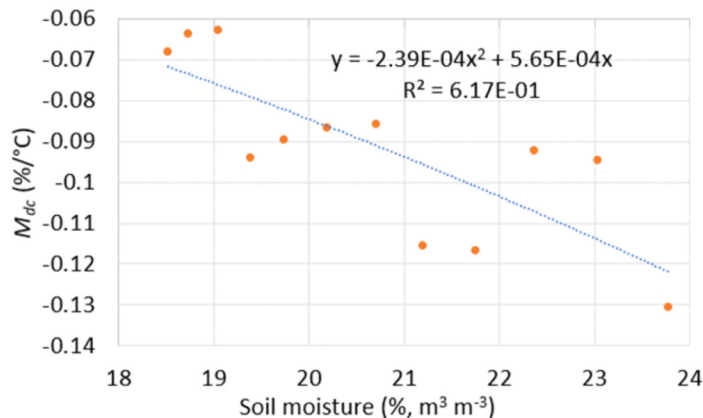
Fig. 6. Temperature coefficient M_{dc} of moisture deviation $\delta\theta$ versus soil moisture.

It was observed that M_{dc} was negative and negatively correlated with moisture content, *i.e.* the lowest absolute M_{dc} values were observed for the lowest values of moisture content.

The observed phenomena may be caused by two main drivers: natural diurnal variation of evaporation and infiltration rates and an influence of temperature on soil apparent dielectric permittivity. Qualitatively similar diurnal changes in soil moisture and temperature was simulated in Chanzy *et al.* (2012) for 2.5 cm soil depth. On the other hand, in the case of high moisture content, the impact of temperature on the soil apparent permittivity is governed by the impact of temperature on free water permittivity, which results in a decrease of permittivity with an increase in temperature. With decreasing moisture the impact of temperature becomes less pronounced, until at a certain moisture value depending on a given soil, no temperature influence is observed, and finally, at even lower moisture contents, the impact of temperature on soil permittivity may be opposite (Skierucha, 2009). If no temperature correction is applied, this would result in measurement errors. The separation of the two mentioned phenomena with the use of laboratory temperature calibrations, application of soil water and energy transfer models and machine learning algorithms may enable development of accurate correction functions that would increase the measurement accuracy of soil moisture monitoring systems.

4. CONCLUSIONS

The developed system and methodology of the data processing enabled to determine and analyse apparent diurnal soil moisture changes during the period of soil drying. The obtained results highlight the need of applying an adequate temperature correction in order to remove the influence of temperature on soil dielectric permittivity, which would enable collection of accurate data for modelling of transfer of water and energy in the soil and in the soil-plant-atmosphere continuum. The developed meas-

urement system, from hardware to visualization, provides potential for future optimization. Based on the determined temperature coefficient, it will be possible to implement an intelligent moisture correction algorithm on the IoT server. Additionally, by preparing predictive algorithms to optimise the frequency of TDR measurements at different soil depths, it will be possible to increase the energy savings of the measurement system.

Conflicts of interest: The authors declare no conflict of interest.

5. REFERENCES

Cepuder P., and Nolz R., 2007. Irrigation management by means of soil moisture sensor technologies. J. Water Land Develop., 11(1): 79-90. https://doi.org/10.2478/v10025-000-0007-0.

Chanzy A., Gaudu J.C., and Marloie O., 2012. Correcting the temperature influence on soil capacitance sensors using diurnal temperature and water content cycles. Sensors (Switzerland) 12(7): 9773-90. https://doi.org/10.3390/s120709773.

Chen Y., and Or D., 2006. Effects of {Maxwell-Wagner} polarization on soil complex dielectric permittivity under variable temperature and electrical conductivity. Water Resour. Res., 42(6). https://doi.org/10.1029/2005wr004590.

Cicioğlu M. and Çalhan A., 2021. Smart agriculture with internet of things in cornfields. Computers Electrical Eng., 90, 106982, https://doi.org/10.1016/j.compeleceng.2021.106982

Gałęzewski L., Jaskulska I., Jaskulski D., Lewandowski A., Szypłowska A., Wilczek A., and Szczepańczyk M., 2021. Analysis of the need for soil moisture, salinity and temperature sensing in agriculture: A case study in Poland. Scientific Reports, 11(1): 16660. https://doi.org/10.1038/s41598-021-96182-1.

Gałęzewski L., Jaskulska I., Kotwica K., and Lewandowski Ł., 2022. The dynamics of soil moisture and temperature – strip-till *vs*. plowing – A case study. Agronomy, 13(1): 83. https://doi.org/10.3390/agronomy13010083.

Goap A., Sharma D., Shukla A.K., and Rama Krishna C., 2018. An IoT based smart irrigation management system using

machine learning and open source technologies. Computers and Electronics in Agriculture, 155 (October): 41-49. https://doi.org/10.1016/j.compag.2018.09.040.

González-Teruel J.D., Torres-Sánchez R., Blaya-Ros P.J., Toledo-Moreo A.B., Jiménez-Buendía M., and Soto-Valles F., 2019. Design and calibration of a low-cost SDI-12 soil moisture sensor. Sensors, 19(3), 491, https://doi.org/10.3390/s19030491

Gong Y., Cao Q., and Sun Z., 2003. The effects of soil bulk density, clay content and temperature on soil water content measurement using time-domain reflectometry. Hydrological Processes, 17(18): 3601-6314. https://doi.org/10.1002/hyp.1358.

Nasar M. and Kausar M.A., 2019. Suitability of influxdb database for iot applications. Int. J. Innovative Technol. Exploring Eng., 8(10), 1850-1857. https://doi.org/10.35940/ijitee.J9225.0881019

Or D. and Wraith J.M., 1999. Temperature effects on soil bulk dielectric permittivity measured by time domain reflectometry: A physical model. Water Resour. Res., 35(2), 371-83. https://doi.org/10.1029/1998WR900008.

Robinson D.A., Campbell C.S., Hopmans J.W., Hornbuckle B.K., Jones S.B., Knight R., Ogden F., Selker J., and Wendroth O., 2008. Soil moisture measurement for ecological and hydrological watershed-scale observatories: A review. Vadose Zone J., 7(1): 358-89. https://doi.org/10.2136/vzj2007.0143.

Skierucha W., 2009. Temperature dependence of time domain reflectometry-measured soil dielectric permittivity. J. Plant Nutrition Soil Sci., 172(2): 186-93.

Skierucha W., Wilczek A., Szypłowska A., Sławiński C., and Lamorski K., 2012. A TDR-based soil moisture monitoring system with simultaneous measurement of soil temperature and electrical conductivity. Sensors (Switzerland), 12(10). https://doi.org/10.3390/s121013545.

Szypłowska A., Lewandowski A., Kafarski M., Szerement J., Wilczek A., Budzeń M., Majcher J., and Skierucha W., 2023. Influence of Temperature on Soil Dielectric Spectra in the 20 MHz – 3 GHz Frequency Range. IEEE Trans. Geoscience Remote Sensing, 61(1): 1-1. https://doi.org/10.1109/tgrs.2023.3313235.

Tan P., Gebremariam E.T., Rahman Md S., Salman H., and Xu H., 2022. Design and implementation of soil moisture monitoring and irrigation system based on ARM and IoT. Procedia Computer Sci., 208: 486-93. https://doi.org/10.1016/j.procs.2022.10.067.

Ullah R., Waseem Abbas A., Ullah M., Ullah Khan R., Ullah Khan I., Aslam N., and Aljameel S.S., 2021. EEWMP: An IoT-based energy-efficient water management platform for smart irrigation. Scientific Programming 2021. https://doi.org/10.1155/2021/5536884.

Vaz Carlos M.P., Jones S., Meding M., and Tuller M., 2013. Evaluation of standard calibration functions for eight electromagnetic soil moisture sensors. Vadose Zone J., 12(2): 1-16. https://doi.org/10.2136/vzj2012.0160.

Vereecken H., Huisman J., Bogena H., Vanderborght J., Vrugt J., and Hopmans J.W., 2008. On the value of soil moisture measurements in Vadose Zone Hydrology: A review. Water Resour. Res., 44 (October): 1-21. https://doi.org/10.1029/2008WR006829.

Wagner N., Emmerich K., Bonitz F., and Kupfer K., 2011. Experimental investigations on the frequency- and temperature-dependent dielectric material properties of soil. IEEE Trans. Geoscience Remote Sensing, 49(7): 2518-30.